Acc. Chem. Res. **1998,** *31,* 351−361

NMR and Spin Relaxation in Dimers

VALERIA CLEMENTI† AND
CLAUDIO LUCHINAT*,‡

Department of Soil Science and Plant Nutrition, P.le delle Cascine 28, and Department of Chemistry, Via Gino Capponi 7, University of Florence, Florence, Italy

Received April 29, 1997

1. Introduction

Relaxation is the return of a system to equilibrium after a perturbation. Many spectroscopies owe their existence to the fact that relaxation occurs on a favorable time scale. Here we only deal with *spin relaxation*, i.e., the return to equilibrium of the projection of the magnetic moment of a large number of spins along a magnetic field (*longitudinal* relaxation) or perpendicular to it (*transverse* relaxation). Electron and/or nuclear spin relaxation phenomena are crucial to all magnetic resonance spectroscopies. An important technique like magnetic resonance imaging is based on differences in nuclear relaxation between and within different tissues and organs. These differences provide the contrast needed for the image.

Both electron and nuclear spins relax by coupling (i.e., exchanging energy) with their lattice (the lattice includes all the degrees of freedom of all molecules, including the ones containing the spins, which can induce transitions between energy states in the investigated spin population), as shown in Figure 1A,B (in some instances, also by coupling among spins within the spin system). Electron−lattice coupling is efficient, whereas nucleus−lattice coupling is inefficient. However, nuclei close to unpaired electrons may exchange energy with them relatively well (Figure 1C), and their relaxation is enhanced. Finally, unpaired electrons on different centers can also relax each other. This interaction has consequences on the ability of nuclei to relax nuclei (Figure 1D). In this Account we will briefly summarize the principles of electron and nuclear relaxation, and then focus on nuclear relaxation in dimers, highlighting how their favorable electronic properties make them suitable for NMR investigations.

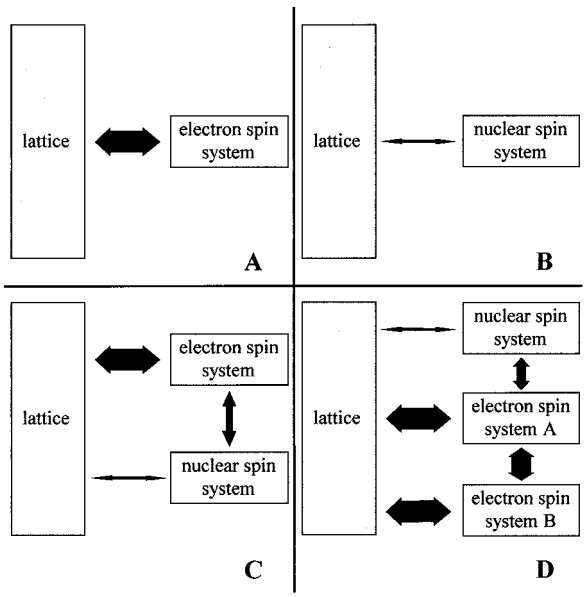

FIGURE 1. Energy exchange between spin systems and the lattice, and between different spin systems. The size of the arrows indicates the efficiency of the exchange.

2. How Spins Relax

A spin transition may be induced by fluctuations of local magnetic fields in the lattice arising, for instance, by random motions of electric charges or of magnetic moments. These random fluctuations generate a whole spectrum of frequencies ranging from zero to τ_c^{-1}, where τ_c is the characteristic *correlation time* of the fluctuations. If the frequency of a spin transition, ω, is contained in the spectrum, relaxation occurs. The shorter the τ_c, the broader the spectrum of frequencies covered, but the smaller the power available at each particular frequency, as illustrated by the *spectral density function* $J(\omega,\tau_c)$ (Figure 2):

$$J(\omega,\tau_c) = \frac{\tau_c}{1 + \omega^2\tau_c^2} \qquad (1)$$

For a given spin transition frequency, ω, the most efficient fluctuations are those with a correlation time $\tau_c \cong \omega^{-1}$, i.e., $J(\omega,\tau_c)_{max} = \tau_c/2$.

The relaxation efficiency also depends on the square of the energy fluctuation amplitude, E, that is usually orders of magnitude larger for electrons than for nuclei. Typical ranges of electron relaxation rates, R^S, and nuclear relaxation rates, R^I, are shown in Figure 3.

Valeria Clementi was born in Ancona (1968) and graduated in physics (1994) and specialized in health physics (1996) at the University of Bologna. She then joined the Florence NMR laboratory with an industry research grant on relaxometry and MRI contrast agents, and is now working on the theory of water−biomolecules interaction.

Claudio Luchinat was born in Florence (1952) and graduated in chemistry (1976), and held a CNR grant (1978−1981) and a tenure of Researcher (1981−1986) position at the University of Florence. He was appointed full Professor at the University of Bologna (1986−1996) and again at the University of Florence (1996−). He received the Nasini (1989) and Federchimica (1994) awards and the European medal for Biological Inorganic Chemistry (1996). He has contributed over 270 publications in inorganic and bioinorganic chemistry and NMR spectroscopy, and three books on relaxation and NMR of paramagnetic systems.

* To whom correspondence should be addressed. Phone: +39-55-3288200. Fax: +39-55-333273. E-mail: claudio@risc1.lrm.fi.cnr.it.
† Department of Chemistry.
‡ Department of Soil Science and Plant Nutrition.

S0001-4842(96)00159-8 CCC: $15.00
Published on Web 05/30/1998

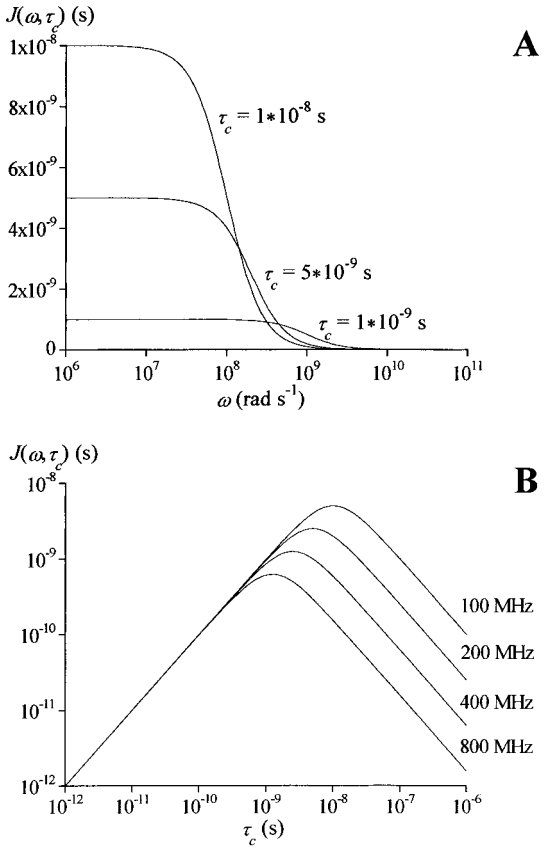

FIGURE 2. Spectral density function $J(\omega,\tau_C)$ (eq 1) as a function of ω (A) for three different values of τ_C and (B) as a function of τ_C for different ν values ($\nu = \omega/2\pi$).

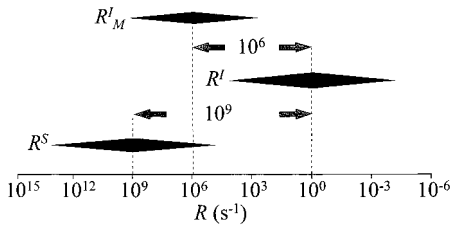

FIGURE 3. Typical ranges of relaxation rates for electrons (R^S), nuclei (in diamagnetic systems R^I), and nuclei interacting with unpaired electrons (R^I_M).

3. Electron-Nucleus Interactions

Nuclear relaxation may be dramatically enhanced by interactions with the large electron spin magnetic moment.[1] The enhancement can be as high as 10^6 (Figure 3). Clearly, nuclear relaxation is a very sensitive reporter of electron−nucleus interactions.

3.1. Dipolar Relaxation. Nuclear relaxation can be induced by fluctuations of the electron spin dipolar field.[2] The dipolar interaction energy decays with r_{IS},[3] where r_{IS} is the electron−nucleus distance, and therefore nuclear relaxation decays with r_{IS}.[6] Three main motions cause energy fluctuations: (1) changes in distance between the two spin vectors; (2) changes in their reciprocal orientation; (3) changes in the sign of the electron spin vectors. The interspin distance can change, for instance, due to chemical exchange, the correlation time being the lifetime of the adduct, τ_M. The reciprocal orientation of the two vectors, both assumed aligned along the external field, changes upon rotation of the molecule, with correlation time τ_R. Finally, the sign of the electron spin vector changes because of electron relaxation: the correlation time, τ_S, is the inverse of the electron relaxation rate, R^S.

The overall correlation time, τ_c, is defined as

$$\tau_c^{-1} = \tau_M^{-1} + \tau_R^{-1} + \tau_S^{-1} \qquad (2)$$

i.e., shorter than the shortest of the three correlation times. When one is much shorter than the others, it effectively dominates τ_c. When τ_S dominates, distinction is made between the longitudinal τ_{S1} and transverse τ_{S2} electronic relaxation times. The case of τ_S being the shortest correlation time is particularly interesting for this Account.

3.2. Contact and Curie Relaxation. Contact relaxation originates from the fraction of unpaired electron delocalized on *s*-type orbitals of the nucleus of interest.[3] It is not influenced by the rotation of the molecule, and its correlation time is

$$\tau_c^{-1} = \tau_M^{-1} + \tau_S^{-1} \qquad (3)$$

A third contribution to nuclear relaxation, called Curie relaxation,[4] is given by the interaction of the nuclear spin with the time-averaged electron magnetic moment, that is small but different from zero because of the slightly longer time that an electron spin spends in the lower spin state.[5,6] Its correlation time is independent of τ_S:

$$\tau_c^{-1} = \tau_M^{-1} + \tau_R^{-1} \qquad (4)$$

This contribution is only important when $\tau_S \ll \tau_R, \tau_M$.

The relevant equations for longitudinal (R^I_{1M}) and transverse (R^I_{2M}) nuclear relaxation in paramagnetic systems (eqs E1−E6)[1−7] are summarized in Figure 4.

4. Electron Relaxation

Electrons can efficiently couple with the orbital magnetic moments arising from their motion around the charged nucleus (*spin−orbit coupling*). In a paramagnetic molecule, in contrast with isolated atoms, the orbital magnetic moment should be quenched because the ground state wave function is a combination of atomic orbitals with opposite m_l values. The quenching is not complete, however, when there are low-lying excited states, and electron relaxation becomes efficient. As shown in Table 1, organic radicals possess the least efficient mechanisms, then come transition-metal ions, and finally lanthanides (except gadolinium), where spin−orbit coupling is so strong that the spin−orbit combination quantum number *J* must be used. Some electron relaxation mechanisms are operative both in the solid state and in solution,[8−10] while others only occur in solution[11,12] (Figure 5).

Table 1 is the basis of the applicability of NMR to paramagnetic systems.[1,4,7] It shows that when τ_S is short, NMR lines can be sharp enough to give high-resolution spectra. Clearly, there is a need to predict the relaxation

dipolar — **electron-induced nuclear relaxation**

$$(E1)\quad R^{1}_{1M} = \frac{2}{15}S(S+1)k\left[\frac{3\tau_{c1}}{1+\omega_I^2\tau_{c1}^2}+\frac{7\tau_{c2}}{1+\omega_S^2\tau_{c2}^2}\right]$$

$$(E2)\quad R^{1}_{2M} = \frac{1}{15}S(S+1)k\left[4\tau_{c1}+\frac{3\tau_{c1}}{1+\omega_I^2\tau_{c1}^2}+\frac{13\tau_{c2}}{1+\omega_S^2\tau_{c2}^2}\right]$$

$$k = \left(\frac{\mu_0}{4\pi}\right)^2\frac{\gamma^2 g_e^2\mu_B^2}{r_{IS}^6}$$

$$\tau_{c1}^{-1} = \tau_{S1}^{-1} + \tau_R^{-1} + \tau_M^{-1} \qquad \tau_{c2}^{-1} = \tau_{S2}^{-1} + \tau_R^{-1} + \tau_M^{-1}$$

contact

$$(E3)\quad R^{1}_{1M} = \frac{2}{3}S(S+1)\left(\frac{A}{\hbar}\right)^2\frac{\tau_{c2}}{1+\omega_S^2\tau_{c2}^2}$$

$$(E4)\quad R^{1}_{2M} = \frac{1}{3}S(S+1)\left(\frac{A}{\hbar}\right)^2\left(\tau_{c1}+\frac{\tau_{c2}}{1+\omega_S^2\tau_{c2}^2}\right)$$

$$\tau_{c1}^{-1} = \tau_{S1}^{-1} + \tau_M^{-1} \qquad \tau_{c2}^{-1} = \tau_{S2}^{-1} + \tau_M^{-1}$$

Curie

$$(E5)\quad R^{1}_{1M} = \frac{2}{5}\alpha\frac{3\tau_c}{1+\omega_I^2\tau_c^2}$$

$$(E6)\quad R^{1}_{2M} = \frac{1}{5}\alpha\left(4\tau_c+\frac{3\tau_c}{1+\omega_I^2\tau_c^2}\right)$$

$$\alpha = \left(\frac{\mu_0}{4\pi}\right)^2\frac{\omega_I^2 g_e^4\mu_B^4 S^2(S+1)^2}{(3kT)^2 r_{IS}^6} \qquad \tau_c^{-1} = \tau_R^{-1} + \tau_M^{-1}$$

dipolar — **electron-induced electron relaxation**

$$(E7)\quad R^{A}_{1B} = \frac{2}{15}k_1\cdot\left(\frac{\tau_{S2B}}{1+(\omega_{SA}-\omega_{SB})^2\tau_{S2B}^2}+\frac{3\tau_{S1B}}{1+\omega_{SA}^2\tau_{S1B}^2}+\frac{6\tau_{S2B}}{1+(\omega_{SA}+\omega_{SB})^2\tau_{S2B}^2}\right)$$

$$(E8)\quad R^{A}_{2B} = \frac{1}{15}k_1\cdot\left(4\tau_{S1B}+\frac{\tau_{S2B}}{1+(\omega_{SA}-\omega_{SB})^2\tau_{S2B}^2}+\frac{3\tau_{S1B}}{1+\omega_{SA}^2\tau_{S1B}^2}+\frac{6\tau_{S2B}}{1+(\omega_{SA}+\omega_{SB})^2\tau_{S2B}^2}+\frac{6\tau_{S1B}}{1+\omega_{SB}^2\tau_{S1B}^2}\right)$$

contact

$$(E9)\quad R^{A}_{1B} = \frac{2}{3}S_B(S_B+1)\left(\frac{J}{\hbar}\right)^2\frac{\tau_{S2B}}{1+(\omega_{SA}-\omega_{SB})^2\tau_{S2B}^2}$$

$$(E10)\quad R^{A}_{2B} = \frac{1}{3}S_B(S_B+1)\left(\frac{J}{\hbar}\right)^2\left(\tau_{S1B}+\frac{\tau_{S2B}}{1+(\omega_{SA}-\omega_{SB})^2\tau_{S2B}^2}\right)$$

$$k_1 = \left(\frac{\mu_0}{4\pi}\right)^2\left(\frac{1}{\hbar}\right)^2\frac{g_e^4\mu_B^4 S_B(S_B+1)}{\langle r_{A,B}^3\rangle^2}$$

dipolar — **dimer-induced nuclear relaxation**

$$(E11)\quad R^{1}_{1MA,B} = \frac{2}{15}k\sum_i\left[C_{iA,B}^2 k_2\cdot\left(\frac{7\tau_{c2i}}{1+\omega_S^2\tau_{c2i}^2}+\frac{3\tau_{c1i}}{1+\omega_I^2\tau_{c1i}^2}\right)/k_3\right]$$

$$(E12)\quad R^{1}_{2MA,B} = \frac{1}{15}k\sum_i\left[C_{iA,B}^2 k_2\cdot\left(4\tau_{c1i}+\frac{13\tau_{c2i}}{1+\omega_S^2\tau_{c2i}^2}+\frac{3\tau_{c1i}}{1+\omega_I^2\tau_{c1i}^2}\right)/k_3\right]$$

$$\tau_{c1i}^{-1} = \tau_{S1i}^{-1} + \tau_R^{-1} + \tau_M^{-1} \qquad \tau_{c2i}^{-1} = \tau_{S2i}^{-1} + \tau_R^{-1} + \tau_M^{-1}$$

contact

$$(E13)\quad R^{1}_{1MA,B} = \frac{2}{3}\frac{A_{A,B}^2}{\hbar^2}\sum_i\left(C_{iA,B}^2 k_2\cdot\frac{\tau_{c2i}}{1+\omega_S^2\tau_{c2i}^2}\right)/k_3$$

$$(E14)\quad R^{1}_{2MA,B} = \frac{1}{3}\frac{A_{A,B}^2}{\hbar^2}\sum_i\left(C_{iA,B}^2 k_2\cdot\left(\tau_{c1i}+\frac{\tau_{c2i}}{1+\omega_S^2\tau_{c2i}^2}\right)\right)/k_3$$

$$k_2 = S'_i(S'_i+1)(2S'_i+1)\exp\left(\frac{-E_i}{kT}\right)$$

$$k_3 = \sum_i\left((2S'_i+1)\exp\left(\frac{-E_i}{kT}\right)\right)$$

$$\tau_{c1i}^{-1} = \tau_{S1i}^{-1} + \tau_M^{-1} \qquad \tau_{c2i}^{-1} = \tau_{S2i}^{-1} + \tau_M^{-1}$$

Curie

$$(E15)\quad R^{1}_{1MA,B} = \frac{2}{5}\frac{k}{(3kT)^2}\sum_i\left[C_{iA,B}^2 S'(S'+1)k_2\cdot\left(\frac{3\tau_c}{1+\omega_I^2\tau_c^2}\right)/k_3\right]$$

$$(E16)\quad R^{1}_{2MA,B} = \frac{1}{5}\frac{k}{(3kT)^2}\sum_i\left[C_{iA,B}^2 S'(S'+1)k_2\cdot\left(4\tau_c+\frac{3\tau_c}{1+\omega_I^2\tau_c^2}\right)/k_3\right]$$

$$\tau_c^{-1} = \tau_R^{-1} + \tau_M^{-1}$$

$$C_{iA,B} = \left[S'_i(S'_i+1) \pm S_A(S_A+1) \mp S_B(S_B+1)\right]/\left[2S'_i(S'_i+1)\right]$$

γ_I = nuclear magnetogyric ratio, g_e = electron g-factor, μ_B = electron Bohr-magneton, $\hbar$ = Plank's costant, A = electron-nuclear contact coupling costant, J = electron-electron contact coupling costant, k = Boltzmann costant. All other symbols are defined in the text.

FIGURE 4. Relevant spin relaxation equations.

behavior of the electron spin also in the presence of electron−electron interactions.

5. Electron−Electron Interactions

Not unexpectedly, an electron spin can also relax by coupling with a neighboring electron spin. More and more systems of chemical or biochemical interest are synthesized or discovered, where two (or more) paramagnetic centers are close in space or even connected through bonds. Coupling between electron spins can thus occur, and electron relaxation can be dramatically affected.

The equations for dipolar and contact relaxation[1] (eqs E7−E10, Figure 4) are similar to those for nuclear relaxation (eqs E1−E4). However, there is a limit to their

Table 1. Electronic Relaxation Times, τ_S, of Monomeric Paramagnetic Systems and Resulting Nuclear Relaxation Rates, $R^I_{1,2M}$[a]

paramagnetic system	S	τ_S (s)	$R^I_{1,2M}$
organic radicals	1/2	10^{-6}–10^{-8}	300–500
Ti^{3+}	1/2	10^{-10}–10^{-11}	40–300
VO^{2+}	1/2	$\sim10^{-8}$	300–500
V^{3+}	1	$\sim10^{-11}$	100–150
V^{2+}	3/2	$\sim10^{-9}$	1500–2000
Cr^{3+}	3/2	5×10^{-9} to 5×10^{-10}	1500–2000
Cr^{2+}	2	10^{-11}–10^{-12}	50–500
Mn^{3+}	2	10^{-10}–10^{-11}	300–2000
Mn^{2+}	5/2	$\sim10^{-8}$	4000–6000
Fe^{3+}(HS)	5/2	10^{-9}–10^{-11}	500–6000
Fe^{3+}(LS)	1/2	10^{-11}–10^{-13}	2–50
Fe^{2+}(HS)	2	10^{-12}–10^{-13}	50–150
Co^{2+}(HS, 5–6_{coord})	3/2	5×10^{-12} to 10^{-13}	20–200
Co^{2+}(HS, 4_{coord})	3/2	$\sim10^{-11}$	200–300
Co^{2+}(LS)	1/2	10^{-9}–10^{-10}	200–400
Ni^{2+}(5–6_{coord})	1	$\sim10^{-12}$	600–700
Ni^{2+}(4_{coord})	1	$\sim10^{-10}$	20–30
Cu^{2+}	1/2	10^{-8}–10^{-9}	300–500
Ru^{3+}	1/2	10^{-11}–10^{-12}	5–50
Re^{3+}	2	10^{-12}–10^{-13}	50–150
Gd^{3+}	7/2	10^{-8}–10^{-9}	5000–15000
paramagnetic system	J	τ_S (s)	$R^I_{1,2M}$
Ce^{3+}	5/2	10^{-13}	7–8
Pr^{3+}	4	3×10^{-13} to 6×10^{-14}	16–30
Nd^{3+}	9/2	2×10^{-13}	20–30
Sm^{3+}	5/2	2×10^{-13} to 5×10^{-14}	0.2–0.6
Eu^{2+}	7/2	$\sim10^{-14}$	300–400
Tb^{3+}	6	2×10^{-13}	800–1000
Dy^{3+}	15/2	1×10^{-12} to 4×10^{-13}	1100–1500
Ho^{3+}	8	8×10^{-13} to 2×10^{-13}	1100–1500
Er^{3+}	15/2	8×10^{-13} to 3×10^{-13}	700–1000
Tm^{3+}	6	5×10^{-13}	300–400
Yb^{3+}	7/2	5×10^{-13} to 2×10^{-13}	50–70

[a] Calculated at 298 K, an 800 MHz proton Larmor frequency, a 5 Å electron–nucleus distance, $\tau_R = 10^{-10}$ s. For longer τ_R values, Curie relaxation may sizably increase R^I_{2M}.

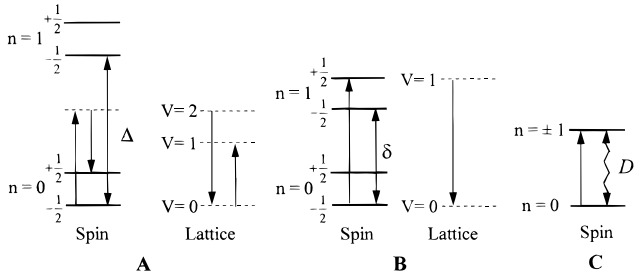

FIGURE 5. Typical solid state (A, B) and solution (C) electron relaxation mechanisms. In the Raman mechanism (A),[8] a spin transition is induced by two lattice transitions, the first of which brings the electron spin to a virtual excited state. In the Orbach mechanism (B),[9] operative when the excited state lies within the thermal bath (<1000 cm^{-1}), direct spin transitions may occur upon promotion of the electron to the excited state. For $S = 1$ or higher, a zero-field splitting D of spin levels may occur, and its modulation by rotation or collisions with solvent molecules may induce relaxation (C).[11,12]

validity (so-called *Redfield limit*[13]), when electron relaxation is concerned: they hold until the amplitude of the energy fluctuation, in frequency units, is smaller than the reciprocal correlation time, i.e., $\langle E^2\rangle^{1/2}/\hbar < \tau_c^{-1}$. Therefore, the resulting relaxation rate can never be larger than the reciprocal correlation time: $R < \tau_c^{-1}$ (Figure 6).

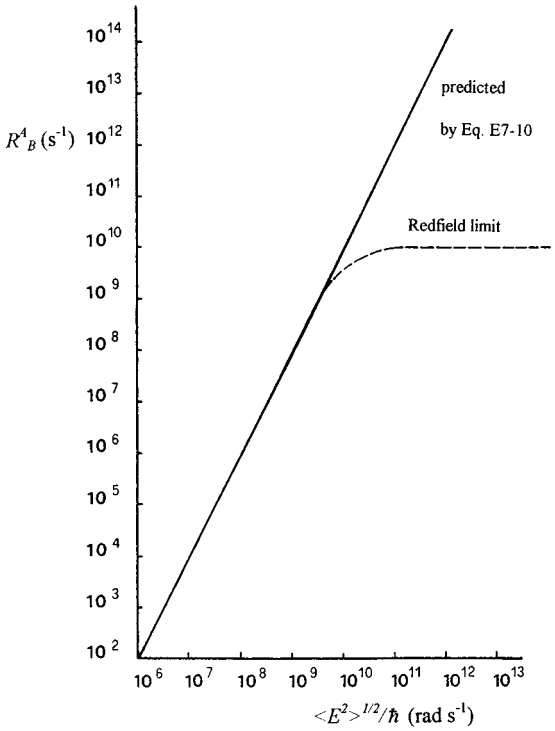

FIGURE 6. Relaxation rate enhancement (R^A_B) of electron spin A by coupling with electron spin B as a function of the coupling energy fluctuation amplitude for $\tau_c = 10^{-10}$ s.[1] Experimentally, R^A_B levels off as it approaches τ_c^{-1}.

Indeed, if the correlation time for the relaxation of spin A is the relaxation time of spin B, the slowly relaxing spin can hardly help the fast relaxing spin to relax (see, however, section 7.2). In contrast, the fast relaxing spin can dramatically enhance relaxation of the slowly relaxing spin.

6. The Fast Relaxes the Slow

6.1. $[Cu–Fe(CN)_6]^-$. Copper(II) is a typical slowly relaxing ion. The NMR lines of its complexes are often too broad to be useful. Conversely, low-spin iron(III) is one of the fastest relaxing ions (Table 1). Tetragonal copper(II) complexes can react with ferricyanide to form dimers (Figure 7A). The ^1H line width of a proton of a copper ligand decreases upon titration with ferricyanide (Figure 7B), as does the copper(II) EPR signal (Figure 7C).[14] Water proton relaxation arising from the copper bound water, measured over a wide range of fields (NMRD), is also decreased (Figure 7D).[15] NMRD allows a direct evaluation of the $J(\omega,\tau)$ spectral density function (cf. Figure 2A).[16] The present data allow us to estimate a τ_S value of 3×10^{-10} s, a factor of 10 shorter than in the absence of ferricyanide.[15] The dipolar contribution (eqs E7 and E8) is too small to account for the observed effect. On the other hand, even a small J value of 1 cm^{-1} in eqs E9 and E10 is enough to explain the observed decrease. Contact relaxation is almost always dominant, as illustrated in Figure 8.

6.2. Cu,Co- and Cu,Ni-SOD. Superoxide dismutases (SOD) are redox metalloproteins whose most likely role

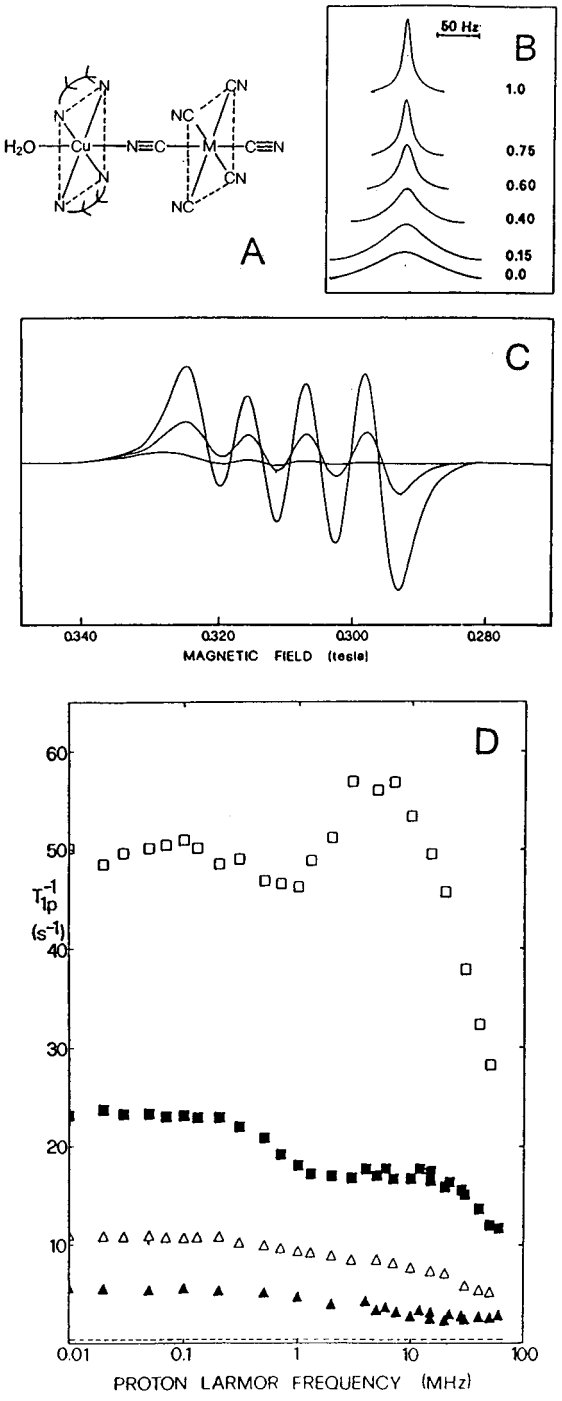

FIGURE 7. (A) Copper(II) bis(ethylenediamine) hexacyanometallate-(III) complex (M = Fe^{3+}, Co^{3+}). (B) Progressive line width decrease of a copper ligand signal. (C) Progressive decrease of the $Cu(en)_2^{2+}$ EPR signal, upon titration with $Fe(CN)_6^{3-}$.[14] (D) Water proton relaxation dispersion (NMRD) of solutions of the adduct of $[Cu(en)_2]^{2+}$ with diamagnetic $[Co(CN)_6]^{3-}$ (□, ■) and with paramagnetic $[Fe(CN)_6]^{3-}$ (○, ●) at 278 K (open symbols) and 298 K (filled symbols).[15]

is to eliminate toxic superoxide ions that form as metabolic side products.[17] They may contain iron, manganese, or copper as the catalytic metal. In the latter case, a zinc(II) ion occupies another metal binding site adjacent to the catalytic copper site (Figure 9). Fast relaxing metal ions substituted for zinc shorten the τ_S of copper, and make SOD amenable to NMR investigations. Among the

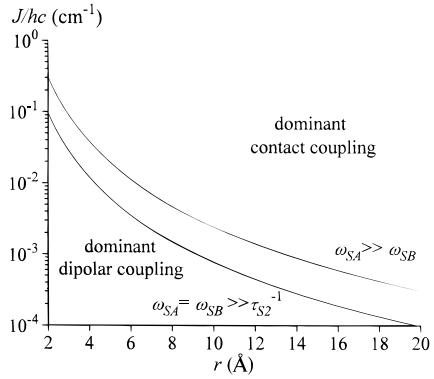

FIGURE 8. Relative efficiency of contact and dipolar electron−electron interactions. The contact interaction is often dominant, except for very small J values and electron−electron distances. The curves separating the two domains are calculated under the two different limiting conditions shown.

several divalent metals that substitute zinc and maintain enzyme activity,[18] nickel(II) and cobalt(II) have favorable relaxation properties (Table 1). Indeed, the Cu,Ni[19] and Cu,Co[20] derivatives display amazingly sharp ^{1}H NMR lines from both the zinc and copper site ligands (Figure 9). In the Cu,Co case, the known intermetal distance (6.3 Å[21]) and J value (17 cm^{-1} [22]) ensure that contact relaxation (eqs E9 and E10) is by far greater than dipolar relaxation (eqs E7 and E8). Indeed, the Redfield limit is already reached here, and τ_S of copper(II) is very close to τ_S of cobalt(II).[23]

Interestingly, the signals from the cobalt and nickel sites are also sharper than those observed when the copper(II) ion is removed, reduced, or substituted with a diamagnetic ion.[23] This effect is not accounted for by eqs E7−E10, but reflects other phenomena to be discussed below.

7. Faster than Fast

Iron and sulfide ions assemble spontaneously under appropriate conditions,[24] giving rise to characteristic cluster structures. This property is believed to have played a crucial role at the early anaerobic stages of life development.[25] Indeed, iron−sulfur-containing proteins (Figure 10) are found throughout evolution, from archebacteria to man. They often act as electron transfer devices.[26] For instance, Fe_2S_2 ferredoxins (Figure 10B) can cycle between a reduced state containing one ferric and one ferrous ion and an oxidized state containing two ferric ions. In both states, the iron ions are magnetically coupled (J = 200 and 400 cm^{-1}, respectively).[27] Each iron is in a pseudotetrahedral environment formed by the two bridging sulfides and two sulfur donors from cysteinate ligands from the protein.

A model for the relaxation properties of monomeric iron in a pseudotetrahedral sulfur donor environment is provided by rubredoxin (Figure 10A). From Table 1, high-spin iron(II) has relatively short electronic relaxation times, while high-spin iron(III) has longer relaxation times. The NMR properties of both are worsened by their high spin quantum numbers (S = 5/2 and S = 2). The ^{1}H NMR spectrum of reduced rubredoxin (Figure 11A)[28] shows

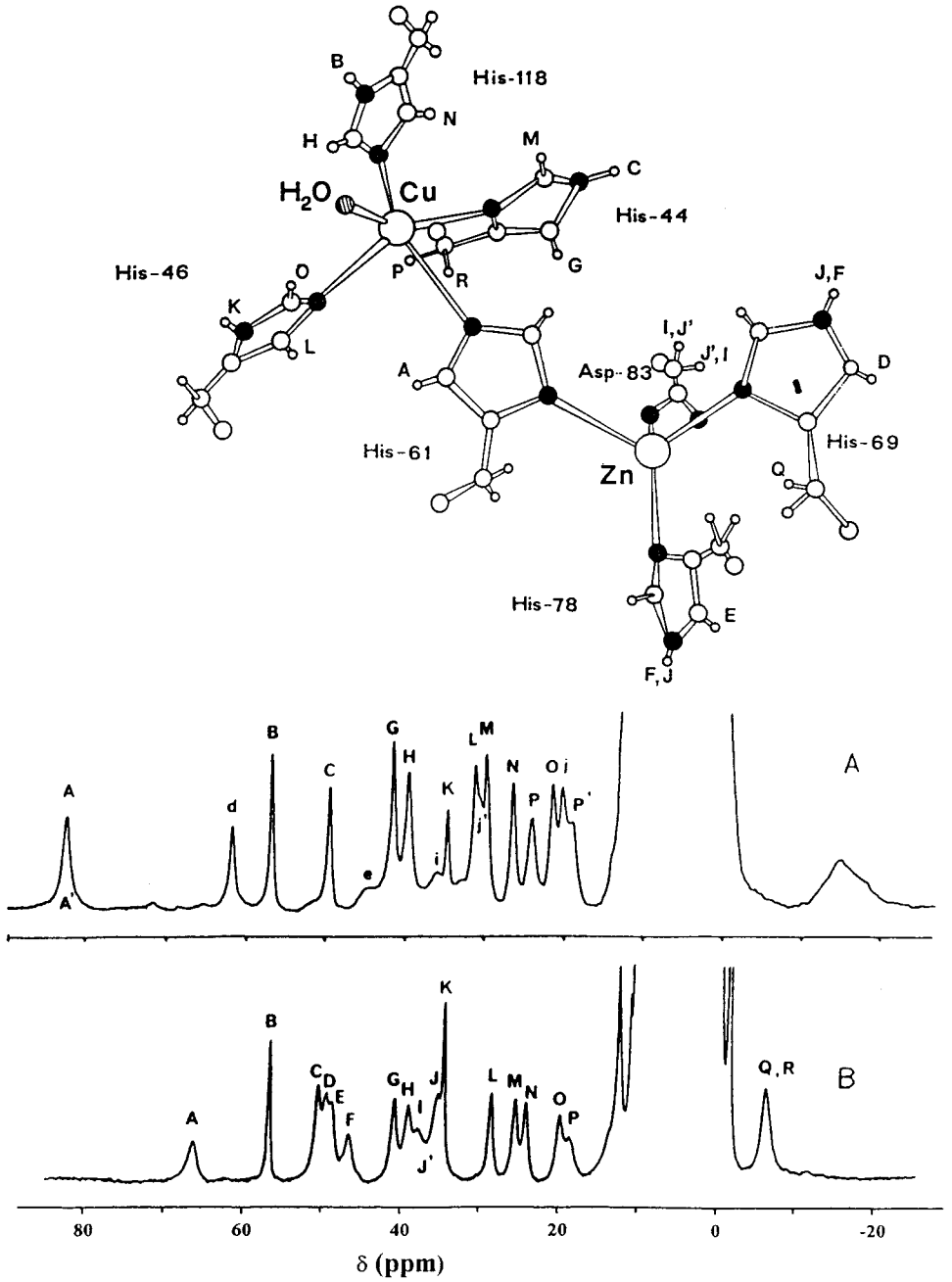

FIGURE 9. Schematic view of the copper and zinc coordination sites in Cu,Zn-SOD, and ^{1}H NMR spectra of the Cu,Ni (A)[19] and Cu,Co (B)[20] derivatives. The assignment of the signals is also shown.

broad downfield-shifted lines belonging to the β-CH_2 protons of the coordinated cysteines. Those of the oxidized species are far too broad, but can be observed in the ^{2}H NMR spectrum (Figure 11B):[28] deuterons have a magnetogyric ratio, γ_I, that is 6.5 times smaller than that of protons, and the paramagnetic effect is 42 times smaller (cf. eqs E1−E6).

The ^{1}H NMR lines of reduced ferredoxin (Figure 11C) are sharper than those of the monomeric counterparts.[29] The spectrum shows two sets of signals, the broader and more shifted (a−d) belonging to the cysteines coordinating the ferric ion and the sharper and less shifted (f−i) belonging to the cysteines coordinating the ferrous ion.[29−31]

Surprisingly, the lines of the ferrous site are much sharper than in reduced rubredoxin. Likewise, the lines in oxidized ferredoxin, containing two iron(III) ions, are also sharper (Figure 11D) than those of oxidized rubredoxin. Apparently, a more complete picture is needed of what happens to nuclear spin systems in significantly magnetically coupled systems.

7.1. Contact Coupling and Energy Levels. When two electron spins, S_A and S_B, are contact-coupled, the energies of the electron spin levels are changed (eq 5),[32] besides

$$E(S') = (1/2)J[S'(S'+1) - S_A(S_A+1) - S_B(S_B+1)]; \quad \Delta E(S') = S'J \quad (5)$$

being split by Zeeman interaction when a magnetic field is applied (Figure 12). Nuclei interacting with either spin A or spin B actually interact with the projection of either

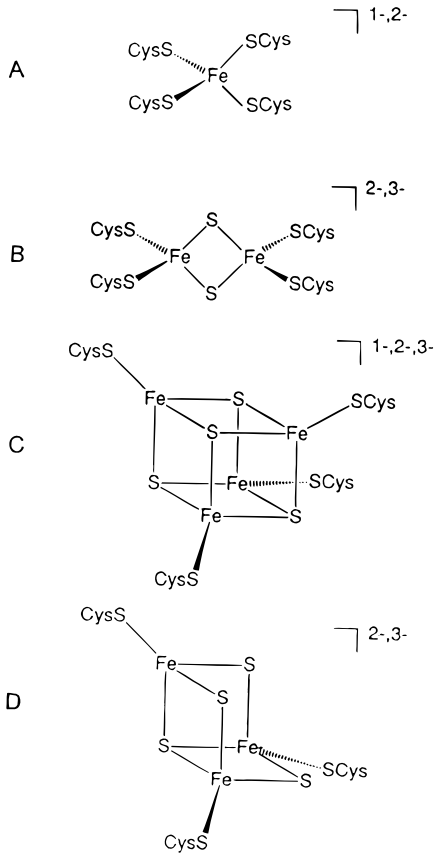

FIGURE 10. Schematic structures of the metal sites in rubredoxin (A) and iron−sulfur proteins containing Fe_2S_2 (B), Fe_4S_4 (C), and Fe_3S_4 (D) clusters.

spin A or spin B of the total spin S', and this projection is different from that of the uncoupled spin. Nuclear relaxation thus depends on the population of the excited S' states, and on whether the largest or smallest S' is lowest in energy (ferro- or antiferromagnetic coupling). Equations E1−E6 have been rederived accordingly (eqs E11−E16 in Figure 4).[1,15,30] The relaxation contribution from each state i is weighted by a coefficient $C_{i,A,B}$ squared. If the ground state has $S' = 0$, the coefficients are also zero. Even with $S' \neq 0$ ground states, if the coupling is antiferromagnetic, the coefficients are smaller than for the excited states, so that if the coupling is sufficiently strong to reduce the Boltzmann population of the more paramagnetic excited states, nuclear relaxation is also decreased.[30,33]

Boltzmann population effects are negligible when $J \ll kT$, because all S' states tend to be equally populated, and ferro- and antiferromagnetic coupled systems have the same behavior. However, the projection effect still remains. In this limit, eqs E11−E16 reduce to eqs E1−E6 multiplied by coefficients $X_{A,B}$ that are related to the average projection of each spin on all S' states:[1,34]

$$X_{A,B} = \frac{\sum_i C^2_{i,A,B}(2S'+1)S'(S'+1)}{S_{A,B}(S_{A,B}+1)\sum_i(2S'+1)} \qquad (6)$$

Analysis of nuclear relaxation in Cu,Co-SOD, for which $J \ll kT$, yields $\tau_S(Cu) = 10^{-11}$ s and $\tau_S(Co) = 5 \times 10^{-12}$ s,[23] again close to each other and to that of isolated cobalt(II) (Redfield limit). Calculations using eqs E11−E16 for oxidized ferredoxin ($S' = 0$, $J = 400$ cm^{-1}) show that the sharpening of the lines with respect to oxidized rubredoxin arises from the decreased Boltzmann population of the paramagnetic excited states. For reduced ferredoxin, the effect is smaller due to (i) the paramagnetic $S' = 1/2$ ground state and (ii) the smaller J value (200 cm^{-1}). When the two spins are different, the coefficients are also different, those of the smaller spin in the lowest states being substantially smaller than those of the larger spin. Calculations using $S_A = 5/2$, $S_B = 2$, and $J = 200$ cm^{-1} predict a factor of 4 in line widths between the two sets of NMR signals.[1,30] This ratio is close enough to the experimental ratio to suggest that τ_S is essentially the same for the two sites (Redfield limit again reached).

However, the calculations also show that τ_S is 1 or 2 orders of magnitude shorter than that of iron(II) in reduced rubredoxin. So other factors besides Boltzmann population effects must be present in this case to explain the sharp NMR lines. Apparently, the picture is not yet complete.

7.2. A Glance beyond the Redfield Limit. It is now apparent that electron−electron interactions are so strong that the Redfield limit is often reached, where no equation for electron relaxation is available. The limiting case of interaction energy much larger than the correlation time, $\langle E^2\rangle^{1/2}/\hbar \gg \tau_c^{-1}$, has recently been considered.[35] As done earlier for nuclear spin−spin coupling and for quadrupolar relaxation[36−39] the approach consists in calculating the line widths and lifetimes in coupled systems, such as those shown in Figure 12, as a function of the relaxation rates of the isolated spins.[36] The calculations result in different electronic relaxation times for each level and for each transition in the coupled system. For instance, the rates for an $S = 1/2-S = 3/2$ pair are shown in Table 2.[35] The relaxation rates for the pair are the sum of the rates of the two spins, weighted by coefficients that differ from one transition to another. When one rate is negligibly small, the rate of the pair only depends on the rate of the fast relaxing system, but is not equal to it. When the fast relaxing system is the one with the largest spin, as for Cu,-Co-SOD, the overall rates are larger than for the isolated fast relaxing ion, while they are smaller when the fast relaxing system is the one with the smallest spin.[35]

The obtained rates can then be used in equations analogous to eqs E11−E14, by introducing for each different S' level the appropriate τ_{S1} (lifetimes) and τ_{S2} (transition line widths). This yields as many $J(\omega,\tau_c)$ spectral density functions as the number of levels and transitions in the system. However, it turns out[35] that the spectral densities containing τ_{S1}, as well as those containing τ_{S2}, can be lumped together, for $J \ll kT$ or $J \gg kT$, using appropriate average τ_{S1} and τ_{S2} values (Table 3). With these values, eqs E11−E14 can be used as such. For instance, the average τ_{S1}^{-1} for the $S = 1/2-S = 3/2$ case, relevant for Cu,Co-SOD, is $(9/16)R(Cu) + (179/96)R(Co)$. As $R(Co)$ and $R(Cu)$ for the isolated ions are 10^{11} and 5 x 10^8 s^{-1}, respectively,[23] τ_{S1}^{-1} is about twice $R(Co)$, or 2 ×

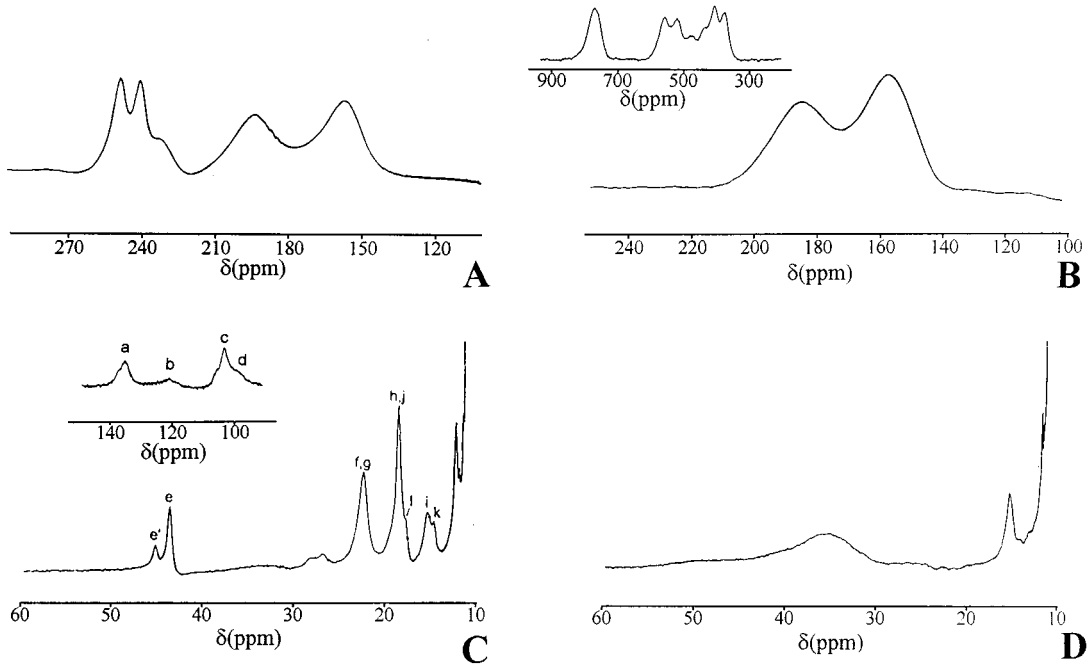

FIGURE 11. NMR spectra of reduced (A) and oxidized (B) rubredoxin,[28] together with reduced (C) and oxidized (D) ferredoxin.[29,31] Spectra A, C, and D are ^{1}H spectra; spectrum B is a ^{2}H spectrum.

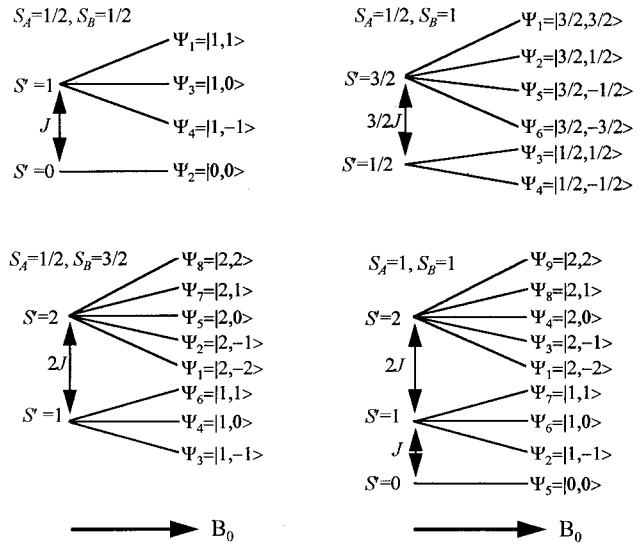

FIGURE 12. Electron spin levels in antiferromagnetically coupled systems. The order of the S' levels is reversed if the coupling is ferromagnetic.

10^{11} s^{-1}. The experimental τ_{S1}^{-1} value ranges between 1 and 2×10^{11} s^{-1}, in good agreement with predictions.

8. Does Slow plus Slow Equal Slow?

The above treatment also applies to homodimers ($S_A = S_B$, $\tau_{S_A} = \tau_{S_B}$). If the electronic relaxation times are the same, they should be unable to strongly influence each other, as shown in Table 3 for $S = 1/2-S = 1/2$ and $S = 1-S = 1$ pairs. As $S_A = S_B$, all $C_{A,B}$ coefficients equal 1/2, and the same holds for the $X_{A,B}$ coefficients. Therefore, we expect a decrease of just a factor of 2 in nuclear relaxation for $J \ll kT$. Of course, for $J \gg kT$ and antiferromagnetic coupling, nuclear relaxation will decrease substantially, as the ground state is diamagnetic ($S' = 0$).

We have already seen that the sharpening of the lines in oxidized Fe_2S_2 ferredoxins is adequately accounted for by Boltzmann population effects. Several other well-behaved examples are known, all involving copper dimers. Cu^{II}-Cu^{II} dimers are currently the subject of active investigation, both as biological moieties (e.g., hemocyanin, tyrosinase, copper dimers in blue proteins, ascorbate oxidase, aminopeptidase) and as synthetic catalysts.[40,41] On the $J \ll kT$ side, negligible τ_S shortening was found for a synthetic dimer (Figure 13A);[34] likewise, the Cu,Cu-SOD derivative yields a τ_S value equal to that of the Cu,Zn-SOD (2×10^{-9} s)[35,42] within less than a factor of 2. On the $J \gg kT$ side, at least three synthetic dimers (Figure 13B−D)[43−45] give NMR lines relatively sharp but consistent with expectations from eqs E11−E16, and τ_S values not much shorter than those of monomeric copper complexes.

However, in an increasing number of copper dimers the NMR lines have been found to be far too sharp to be explained.[43−49] The most striking example is the weakly coupled dimer whose structure and NMR spectra are reported in Figure 14.[49] The corresponding monomer has a "normal" τ_S of 10^{-9} s, while the dimer has a τ_S of 10^{-11} s.

Apparently, new relaxation pathways are sometimes created upon dimer formation. The nature of these pathways has still to be ascertained. A possibility is that the small J value can be modulated by solvent collision more effectively than by τ_S. Calculations using eqs E9 and E10 with a collision correlation time τ_ν of $10^{-11}-10^{-12}$ s suggest that a sizable shortening of τ_S is possible. An alternative[49] is a modulation of the zero-field splitting of

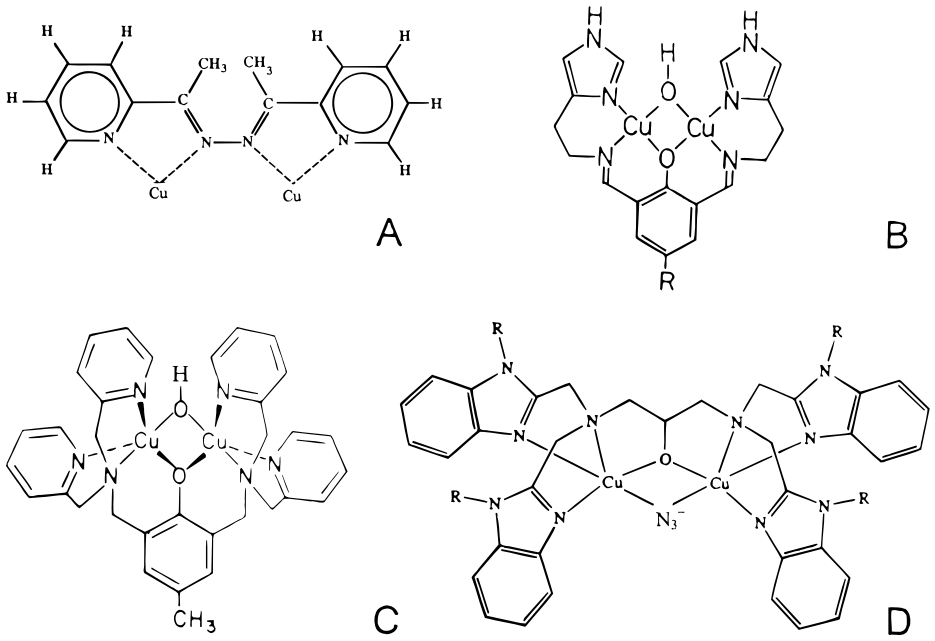

FIGURE 13. Copper(II) dimers with $J \ll kT$ (A)[34] and $J \geq kT$ (B−D).[43−45]

Table 2. Total Line Widths (Off-Diagonal Elements) and Inverse Lifetimes (Diagonal, Bold) for a *J*-Coupled $S_A = 1/2$, $S_B = 3/2$ System[35]

	$\Psi_{1(8)}$	$\Psi_{2(7)}$	$\Psi_{3(6)}$	$\Psi_{4(5)}$
$\Psi_{1(8)}$	$\mathbf{(1/2)}\boldsymbol{R_A} + \mathbf{(3/2)}\boldsymbol{R_B}$	$(5/8)R_A + (21/8)R_B$	$(7/8)R_A + (57/32)R_B$	$(3/4)R_A + (15/4)R_B$
$\Psi_{2(7)}$	$(5/8)R_A + (21/8)R_B$	$\mathbf{(11/16)}\boldsymbol{R_A} + \mathbf{(51/16)}\boldsymbol{R_B}$	$(13/16)R_A + (87/32)R_B$	$(9/8)R_A + (15/4)R_B$
$\Psi_{3(6)}$	$(7/8)R_A + (57/32)R_B$	$(13/16)R_A + (87/32)R_B$	$\mathbf{(11/16)}\boldsymbol{R_A} + \mathbf{2}\boldsymbol{R_B}$	$(3/4)R_A + (117/32)R_B$
$\Psi_{4(5)}$	$(3/4)R_A + (15/4)R_B$	$(9/8)R_A + (15/4)R_B$	$(3/4)R_A + (117/32)R_B$	$\mathbf{(3/4)}\boldsymbol{R_A} + \mathbf{(15/4)}\boldsymbol{R_B}$
$\Psi_{5(4)}$	$(3/4)R_A + (15/4)R_B$	$(9/8)R_A + (15/4)R_B$	$(3/4)R_A + (117/32)R_B$	$\mathbf{(3/4)}\boldsymbol{R_A} + \mathbf{(15/4)}\boldsymbol{R_B}$
$\Psi_{6(3)}$	$(5/8)R_A + (177/32)R_B$	$(11/16)R_A + (147/32)R_B$	$\mathbf{(13/16)}\boldsymbol{R_A} + \mathbf{(41/16)}\boldsymbol{R_B}$	$(3/4)R_A + (117/32)R_B$
$\Psi_{7(2)}$	$(7/8)R_A + (39/8)R_B$	$\mathbf{(13/16)}\boldsymbol{R_A} + \mathbf{(69/16)}\boldsymbol{R_B}$	$(11/16)R_A + (147/32)R_B$	$(9/8)R_A + (15/4)R_B$
$\Psi_{8(1)}$	$\boldsymbol{R_A} + \mathbf{6}\boldsymbol{R_B}$	$(7/8)R_A + (39/8)R_B$	$(5/8)R_A + (177/32)R_B$	$(3/4)R_A + (15/4)R_B$

Table 3. Effective Electron Relaxation Rates for *J*-Coupled Systems (A, 1/2−1/2; B, 1/2−1; C, 1/2−3/2; D, 1−1) in the High-Temperature (HT) and Low-Temperature Antiferro- (AF) and Ferromagnetic (F) Coupling Limits[35]

	$S_A = 1/2$, $S_B = 1/2$			$S_A = 1$, $S_B = 1$		
	N-S_A, N-S_B			N-S_A, N-S_B		
	HT	AF	F	HT	AF	F
τ_1^{-1}	$(1/2)R_A + (1/2)R_B$	diamagnetic state	$(1/2)R_A + (1/2)R_B$	$(5/4)R_A + (5/4)R_B$	diamagnetic state	$(23/20)R_A + (23/20)R_B$
τ_2^{-1}	$(3/4)R_A + (3/4)R_B$		$(3/4)R_A + (3/4)R_B$	$(7/4)R_A + (7/4)R_B$		$(69/40)R_A + (69/40)R_B$

$S_A = 1/2$, $S_B = 1$

	N-S_A			N-S_B		
	HT	AF	F	HT	AF	F
τ_1^{-1}	$(107/198)R_A + (112/99)R_B$	$(13/18)R_A + (14/9)R_B$	$(47/90)R_A + (49/45)R_B$	$(73/126)R_A + (77/63)R_B$	$(13/18)R_A + (14/9)R_B$	$(47/90)R_A + (49/45)R_B$
τ_2^{-1}	$(71/99)R_A + (187/99)R_B$	$(7/9)R_A + (7/3)R_B$	$(32/45)R_A + (83/45)R_B$	$(46/63)R_A + (125/63)R_B$	$(7/9)R_A + (7/3)R_B$	$(32/45)R_A + (83/45)R_B$

$S_A = 1/2$, $S_B = 3/2$

	N-S_A			N-S_B		
	HT	AF	F	HT	AF	F
τ_1^{-1}	$(9/16)R_A + (179/96)R_B$	$(11/16)R_A + 2R_B$	$(43/80)R_A + (147/80)R_B$	$(331/560)R_A + (2123/1120)R_B$	$(11/16)R_A + 2R_B$	$(43/80)R_A + (147/80)R_B$
τ_2^{-1}	$(43/48)R_A + (215/64)R_B$	$(3/4)R_A + (117/32)R_B$	$(37/40)R_A + (33/10)R_B$	$(69/80)R_A + (7677/2240)R_B$	$(3/4)R_A + (117/32)R_B$	$(37/40)R_A + (33/10)R_B$

the $S' = 1$ level,[11,12] arising in turn from J anisotropy.[32] In this case, the system would behave like an isolated $S = 1$ ion, which is often relaxed by this mechanism[50] (Figure 5C). Relaxation efficiency would thus be linked not to the value of J but rather to its ability to be modulated by collision with solvent molecules in solution. Too few well-characterized examples are at hand to confirm the validity of this picture, which at present is only a reasonable working hypothesis. Another mechanism could be derived from the example given in the next section.

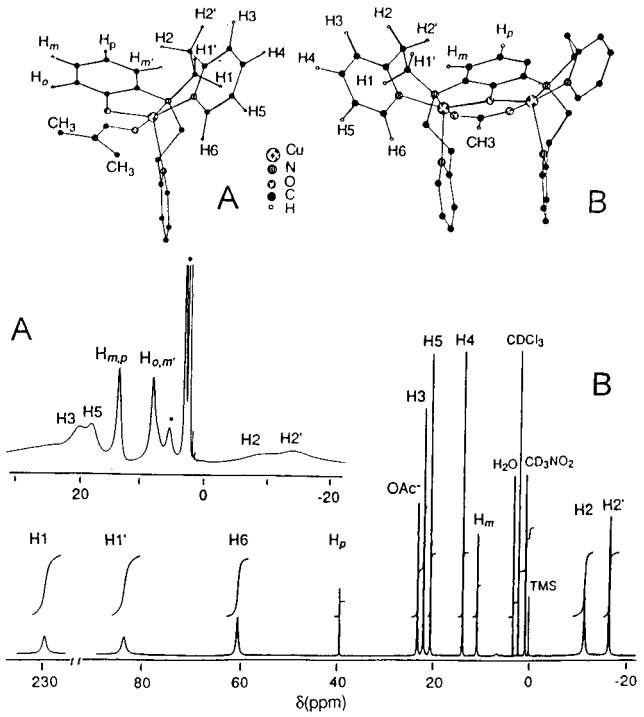

FIGURE 14. Structures and ^{1}H NMR spectra of a copper monomer (A) and the corresponding copper dimer (B).[49] The signal assignment is also shown.

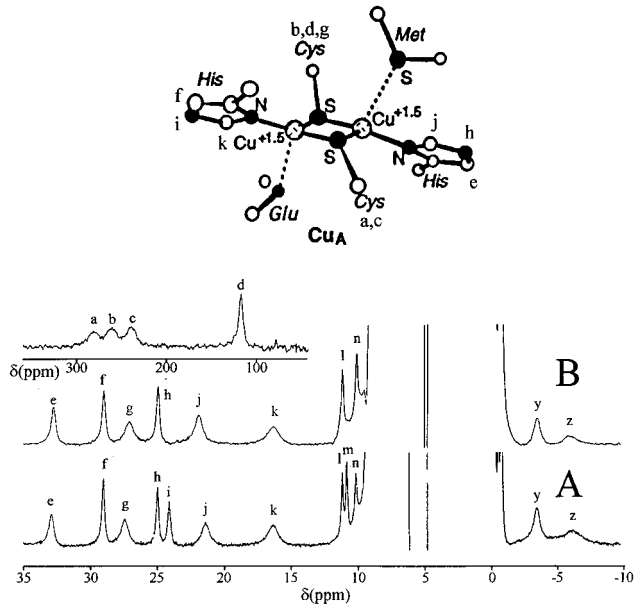

FIGURE 15. Schematic structure of the Cu_A center and ^{1}H NMR spectra at pH 4.5 (A) and 8 (B) of a Cu_A fragment from *T. thermophilus*.[53] The signal assignment is also shown.

9. Sharing One Unpaired Electron

In the last few years, we have witnessed the exciting discovery of the structure of the so-called Cu_A center that is present in nitrous oxide reductase and in subunit II of cytochrome *c* oxidase.[51,52] The center has an electron transfer role and is constituted by two copper ions bridged by two cysteine sulfurs (Figure 15). The reduced form contains two diamagnetic Cu^+ ions, while the oxidized form has one unpaired electron delocalized over the two metals, which are thus $Cu^{1.5+}$. The NMR spectra[53−56] show narrow lines from the copper ligands (Figure 15). The estimated $\tau_S \cong 10^{-11}$ s[53] is comparable to the most striking example among Cu^{2+}−Cu^{2+} dimers shown in section 8. However, in Cu_A there is no magnetic coupling between the two centers, as they contain only one unpaired electron just as an isolated Cu^{2+} ion. Yet its electron relaxation is remarkably more efficient than that of copper(II).

What then makes electron relaxation in Cu_A so efficient? In Cu_A there is considerable orbital overlap between the two copper centers.[57,58] The two highest MOs are antibonding linear combinations of copper d_{xy} and $d_{x^2-y^2}$ and of sulfur p_x and p_y of the Cu_2S_2 moiety. They are nondegenerate, for symmetry reasons, but not far from one another (a few thousand wavenumbers is a reasonable estimate). These two orbitals contain three electrons, so that the higher must be singly occupied. This situation is a typical case where Raman relaxation (Figure 4A) should be efficient.[8,10] Therefore, relaxation in Cu_A may be fast because the dimer structure provides new relaxation mechanisms not available to the monomer.[53,59]

The Cu_A mechanism can possibly be transferred to other dimeric systems, like reduced Fe_2S_2 ferredoxin and possibly some copper(II) dimers: besides the effects on electron relaxation and on the spin energy levels due to the presence of magnetic coupling, additional relaxation mechanisms may be created due to the altered electronic structure of the pair.

10. Concluding Remarks

In order to extract the most information when applying NMR to dimers, we need to understand the principles underlying their electron and nuclear relaxation. Much is now understood, although some challenging puzzles remain. Certainly, we already have a take-home lesson: high-resolution NMR is definitely applicable to dimers when it is applicable to at least one of the constituting monomers. It is often applicable to dimers even when the monomers are not suitable, due either to reduced paramagnetism or to the presence of new dimer-based electron relaxation mechanisms, or both. In all cases, the NMR properties become more favorable. In many cases, the results are striking. Therefore, given the explosion of applications of NMR to monomeric paramagnetic molecules in the past decade, it is easy to predict an even greater success with dimers in the next years.

Finally, a comment on polymetallic systems. Here the theory is largely lacking, but experiments indicate that polymetallic systems containing three or four metal ions are often even more favorable for NMR investigation.[27]

References

(1) Banci, L.; Bertini, I.; Luchinat, C. *Nuclear and electron relaxation. The magnetic nucleus-unpaired electron coupling in solution*; VCH: Weinheim, 1991.
(2) Solomon, I. *Phys. Rev.* **1955**, *99*, 559−565.
(3) Bloembergen, N. *J. Chem. Phys.* **1957**, *27*, 575−596.

(4) Bertini, I.; Luchinat, C. *NMR of paramagnetic molecules in biological systems*; Benjamin/Cummings: Menlo Park, CA, 1986.
(5) Gueron, M. *J. Magn. Reson.* **1975**, *19*, 58−66.
(6) Vega, A. J.; Fiat, D. *Mol. Phys.* **1976**, *31*, 347−362.
(7) Bertini, I.; Luchinat, C. *NMR of paramagnetic substances*; *Coord. Chem. Rev.* Elsevier: Amsterdam, 1996; Vol. 150, pp 1−300.
(8) Van Vleck, J. H. *Phys. Rev.* **1940**, *57*, 426.
(9) Orbach, R. *Proc. R. Soc. London* **1961**, *A264*, 458.
(10) Kivelson, D. *J. Chem. Phys.* **1966**, *45*, 1324−1332.
(11) Bloembergen, N.; Morgan, L. O. *J. Chem. Phys.* **1961**, *34*, 842−850.
(12) Rubinstein, M.; Baram, A.; Luz, Z. *Mol. Phys.* **1971**, *20*, 67−80.
(13) Redfield, A. G. *Adv. Magn. Reson.* **1965**, *1*, 1−32.
(14) Bertini, I.; Luchinat, C.; Mani, F.; Scozzafava, A. *Inorg. Chem.* **1980**, *19*, 1333−1336.
(15) Bertini, I.; Lanini, G.; Luchinat, C.; Mancini, M.; Spina, G. *J. Magn. Reson.* **1985**, *63*, 56−63.
(16) Koenig, S. H.; Brown, R. D., III. *Prog. Nucl. Magn. Reson. Spectrosc.* **1990**, *22*, 487−567.
(17) Sawyer, D.; Valentine, J. S. *Acc. Chem. Res.* **1981**, *14*, 393−400.
(18) Valentine, J. S.; Pantoliano, M. W. In *Copper Proteins*; Spiro, T. G., Ed.; Wiley: New York, 1981; p 291.
(19) Ming, L. J.; Banci, L.; Luchinat, C.; Bertini, I.; Valentine, J. S. *Inorg. Chem.* **1988**, *27*, 4458−4463.
(20) Bertini, I.; Lanini, G.; Luchinat, C.; Messori, L.; Monnanni, R.; Scozzafava, A. *J. Am. Chem. Soc.* **1985**, *107*, 4391−4396.
(21) Tainer, J. A.; Getzoff, E. D.; Beem, K. M.; Richardson, J. S.; Richardson, D. C. *J. Mol. Biol.* **1982**, *160*, 181−217.
(22) Morgenstern-Badarau, I.; Cocco, D.; Desideri, A.; Rotilio, G.; Jordanov, J.; Dupré, N. *J. Am. Chem. Soc.* **1986**, *108*, 300−302.
(23) Bertini, I.; Luchinat, C.; Piccioli, M. *Prog. Nucl. Magn. Reson. Spectrosc.* **1994**, *26*, 91−141.
(24) Holm, R. H.; Kennepohl, P.; Solomon, E. I. *Chem. Rev.* **1996**, *96*, 2239−2314.
(25) Wächtershäuser, G. *Proc. Natl. Acad. Sci. U.S.A.* **1990**, *87*, 200−204.
(26) Anonymous. Cammack, R., Sykes, A. G., Eds.; Academic Press: San Diego, 1992.
(27) Bertini, I.; Ciurli, S.; Luchinat, C. In *Structure and Bonding*; Springer-Verlag: Berlin, Heidelberg, 1995; Vol. 83, pp 1−54.
(28) Xia, B.; Westler, W. M.; Cheng, H.; Meyer, J.; Moulis, J.-M.; Markley, J. L. *J. Am. Chem. Soc.* **1995**, *117*, 5347−5350.
(29) Bertini, I.; Lanini, G.; Luchinat, C. *Inorg. Chem.* **1984**, *23*, 2729−2730.
(30) Banci, L.; Bertini, I.; Luchinat, C. *Struct. Bond.* **1990**, *72*, 113−135.
(31) Benini, S.; Ciurli, S.; Luchinat, C. *Inorg. Chem.* **1995**, *34*, 417−420.
(32) Bencini, A.; Gatteschi, D. *Electron Paramagnetic Resonance of Exchange-Coupled Systems*; Springer-Verlag: Berlin, 1990.
(33) Luchinat, C.; Ciurli, S. *Biol. Magn. Reson.* **1993**, *12*, 357−420.
(34) Owens, C.; Drago, R. S.; Bertini, I.; Luchinat, C.; Banci, L. *J. Am. Chem. Soc.* **1986**, *108*, 3298−3303.
(35) Bertini, I.; Galas, O.; Luchinat, C.; Parigi, G.; Spina, G. *J. Magn. Reson.* **1998**, *130*, 33−44.
(36) Freeman, R.; Wittekoek, S.; Ernst, R. R. *J. Chem. Phys.* **1970**, *52*, 1529−1544.
(37) Ainbinder, N. E.; Shaposhnikov, I. G. *Adv. Nucl. Quad. Reson.* **1978**, *3*, 67−130.
(38) Halle, B. *Prog. Nucl. Magn. Reson. Spectrosc.* **1996**, *28*, 137−159.
(39) Bruschweiler, R.; Case, D. A. *Phys. Rev. Lett.* **1994**, *72*, 940−943.
(40) Kitajima, N.; Moro-oka, Y. *Chem. Rev.* **1994**, *94*, 737−757.
(41) Karlin, K. D.; Murthy, N. N.; Mahroof-Tahir, M. *J. Am. Chem. Soc.* **1993**, *115*, 10404−10405.
(42) Bertini, I.; Banci, L.; Brown, R. D., III; Koenig, S. H.; Luchinat, C. *Inorg. Chem.* **1988**, *27*, 951−953.
(43) Maekawa, M.; Kitagawa, S.; Munakata, M.; Masuda, H. *Inorg. Chem.* **1989**, *28*, 1904−1909.
(44) Holz, R. C.; Brink, J. M. *Inorg. Chem.* **1994**, *33*, 4609−4610.
(45) Mandal, P. K.; Manoharan, P. T. *Inorg. Chem.* **1995**, *34*, 270.
(46) Lubben, L.; Hage, R.; Meetsma, A.; Byma, K.; Feringa, B. L. *Inorg. Chem.* **1995**, *34*, 2217.
(47) Satcher, J. H.; Balch, A. L. *Inorg. Chem.* **1995**, *34*, 3371.
(48) Brink, J. M.; Rose, R. A.; Holz, R. C. *Inorg. Chem.* **1996**, *35*, 2878.
(49) Murthy, N. N.; Karlin, K. D.; Bertini, I.; Luchinat, C. *J. Am. Chem. Soc.* **1997**, *119*, 2156−2162.
(50) Kowalewski, J. *Annu. Rep. NMR Spectrosc.* **1987**, *23*,
(51) Kroneck, P. M. H.; Antholine, W. E.; Riester, J.; Zumft, W. G. *FEBS Lett.* **1988**, *242*, 70−74.
(52) Iwata, S.; Ostermeier, C.; Ludwig, B.; Michel, H. *Nature* **1995**, *376*, 660−669.
(53) Bertini, I.; Bren, K. L.; Clemente, A.; Fee, J. A.; Gray, H. B.; Luchinat, C.; Malmström, B. G.; Richards, J. H.; Sanders, D.; Slutter, C. E. *J. Am. Chem. Soc.* **1996**, *46*, 11658−11659.
(54) Dennison, C.; Berg, A.; de Vries, S.; Canters, G. W. *FEBS Lett.* **1996**, *394*, 340−344.
(55) Luchinat, C.; Soriano, A.; Djinovic Carugo K.; Saraste, M.; Malmström, B. G.; Bertini, I. *J. Am. Chem. Soc.* **1997**, *119*, 11023−11027.
(56) Dennison, C.; Berg, A.; Canters, G. W. *Biochemistry* **1997**, *36*, 3262−3269.
(57) Farrar, J. A.; Neese, F.; Lappalainen, P.; Kroneck, P. M. H.; Saraste, M.; Zumft, W. G.; Thomson, A. J. *J. Am. Chem. Soc.* **1996**, *118*, 11501−11514.
(58) Williams, K. R.; Gamelin, D. R.; LaCroix, L. B.; Houser, R. P.; Tolman, W. B.; Mulder, T. C.; de Vries, S.; Hedman, B.; Hodgson, K. O.; Solomon, E. I. *J. Am. Chem. Soc.* **1997**, *119*, 613−614.
(59) Pfenninger, S.; Antholine, W. E.; Barr, M. E.; Hyde, J. S.; Kroneck, P. M. H.; Zumft, W. G. *Biophys. J.* **1995**, *69*, 2761−2769.

AR960159+